

## Charge Density of Divalent Metal Cations Determines RNA Stability

Eda Koculi,<sup>†,||</sup> Changbong Hyeon,<sup>‡,§</sup> D. Thirumalai,<sup>\*,‡</sup> and Sarah A. Woodson<sup>\*,†</sup>

Contribution from the T. C. Jenkins Department of Biophysics, Johns Hopkins University, 3400 North Charles Street, Baltimore, Maryland 21218, and Biophysics Program, Institute for Physical Sciences and Technology and Department of Chemistry and Biochemistry, University of Maryland, College Park, Maryland 20742

Received November 9, 2006; E-mail: thirum@glue.umd.edu; swoodson@jhu.edu

**Abstract:** RNA molecules are exquisitely sensitive to the properties of counterions. The folding equilibrium of the *Tetrahymena* ribozyme is measured by nondenaturing gel electrophoresis in the presence of divalent group IIA metal cations. The stability of the folded ribozyme increases with the charge density ( $\zeta$ ) of the cation. Similar scaling is found when the free energy of the RNA folded in small and large metal cations is measured by urea denaturation. Brownian dynamics simulations of a polyelectrolyte show that the experimental observations can be explained by nonspecific ion–RNA interactions in the absence of site-specific metal chelation. The experimental and simulation results establish that RNA stability is largely determined by a combination of counterion charge and the packing efficiency of condensed cations that depends on the excluded volume of the cations.

### Introduction

Divalent metal cations are required for RNAs to fold into their functional 3D structures and for RNA catalysis.<sup>1,2</sup> Understanding how metal ions interact with RNA is important, not only because the metal ions stabilize the folded RNA but also because different counterions alter the dynamics and even the catalytic function of the RNA.<sup>3</sup> Metal ion interactions are difficult to describe quantitatively, however, because the ions interact with each other and with the solvent, as well as with the RNA.<sup>4</sup> Thus, the properties of the ions as well as the structure of the RNA must be considered. In this paper, we report that the stability of the folded *Tetrahymena* ribozyme decreases linearly with the size of hydrated group IIA metal ions, demonstrating that the charge density of the counterions is important for RNA folding.

Metal ions are strongly attracted by the electrostatic potential of an RNA, and folded RNAs that have regions of high negative potential interact even more strongly with counterions than unfolded RNAs.<sup>5</sup> These “nonspecific” interactions account for most of the thermodynamic stabilization of the RNA by metal

ions.<sup>4</sup> Although the majority of metal ions remain hydrated and mobile with respect to the RNA,<sup>6</sup> partially dehydrated ions can directly coordinate the RNA, and such interactions are expected to be selective for an ion size and coordination geometry.<sup>2</sup> In the *Tetrahymena* ribozyme, specific Mg<sup>2+</sup> binding sites have been identified within the catalytic active site<sup>7,8</sup> and in the P5abc subdomain.<sup>9</sup> Despite the importance of binding of metal ions to specific sites on RNA, however, substantial neutralization of the phosphate charge arises from nonspecific condensation of counterions.<sup>4,10</sup>

The ionic radius of a metal cation correlates with many of its chemical and physical properties, such as hydration state, bond energy, and polarizability.<sup>11</sup> Thus, Mg<sup>2+</sup>, a relatively small ion, forms stronger metal–oxygen bonds, is less polarizable, and raises the p*K*<sub>a</sub> of waters in the first hydration sphere more than Sr<sup>2+</sup> or Ba<sup>2+</sup>. Because of these differences in coordination chemistry, the effects of metal ions on RNA structure and folding are often attributed to the energetic cost of dehydrating the metal, or its ability to chelate specific ligands within the RNA.<sup>12</sup>

<sup>†</sup> Johns Hopkins University.

<sup>‡</sup> University of Maryland.

<sup>§</sup> Present address: Center for Theoretical Biological Physics, University of California San Diego, 9500 Gilman Dr., La Jolla, CA 92093.

<sup>||</sup> Present address: Scripps Research Institute, 10550 Torrey Pines Road, MB 203, La Jolla, CA 92037.

(1) Pyle, A. M. *J. Biol. Inorg. Chem.* **2002**, *7*, 679; Fedor, M. J. *Curr. Opin. Struct. Biol.* **2002**, *12*, 289.  
(2) DeRose, V. J. *Curr. Opin. Struct. Biol.* **2003**, *13*, 317.  
(3) Woodson, S. A. *Curr. Opin. Chem. Biol.* **2005**, *9*, 104.  
(4) Draper, D. E.; Grilley, D.; Soto, A. M. *Annu. Rev. Biophys. Biomol. Struct.* **2005**, *34*, 221.  
(5) Hermann, T.; Westhof, E. *Structure* **1998**, *6*, 1303; Misra, V. K.; Draper, D. E. *J. Mol. Biol.* **1999**, *294*, 1135.

(6) Draper, D. E. *RNA* **2004**, *10*, 335.

(7) Piccirilli, J. A.; Vyle, J. S.; Caruthers, M. H.; Cech, T. R. *Nature* **1993**, *361*, 85.

(8) Guo, F.; Gooding, A. R.; Cech, T. R. *Mol. Cell* **2004**, *16*, 351.

(9) Cate, J. H.; Hanna, R. L.; Doudna, J. A. *Nat. Struct. Biol.* **1997**, *4*, 553; Das, R.; Travers, K. J.; Bai, Y.; Herschlag, D. *J. Am. Chem. Soc.* **2005**, *127*, 8272; Basu, S.; Strobel, S. A. *RNA* **1999**, *5*, 1399.

(10) Thirumalai, D.; Lee, N.; Woodson, S. A.; Klimov, D. *Annu. Rev. Phys. Chem.* **2001**, *52*, 751; Record, M. T., Jr.; Anderson, C. F.; Lohman, T. M. *Q. Rev. Biophys.* **1978**, *11*, 103.

(11) Feig, A. L.; Uhlenbeck, O. C., Metal ions and RNA. In *The RNA World*, 2nd ed.; Gesteland, R. F., Cech, T. R., Atkins, J. F., Eds.; Cold Spring Harbor Laboratory Press: Cold Spring Harbor, NY, 2000; p 287.

(12) Dahm, S. C.; Uhlenbeck, O. C. *Biochemistry* **1991**, *30*, 9464; Fang, X. W.; Thiyagarajan, P.; Sosnick, T. R.; Pan, T. *Proc. Natl. Acad. Sci. U.S.A.* **2002**, *99*, 8518; Ennifar, E.; Walter, P.; Dumas, P. *Nucleic Acids Res.* **2003**, *31*, 2671.

In order for RNA to fold, the negative charges on the phosphate groups must be substantially neutralized, which occurs upon counterion condensation.<sup>4</sup> Cations condense onto the RNA backbone if the favorable electrostatic binding energy between the counterion and the phosphate group compensates for the free energy cost due to the loss in translational entropy of the counterions.<sup>13,14</sup> The balance between these forces depends on the valence ( $Z$ ) of the cations. Excluded volume interactions between condensed counterions, however, result in spatial correlations that position any two metal ions at distances greater than the sum of their ionic radii.<sup>15</sup> As both  $Z$  and the volume ( $V$ ) of the ions contribute to the distribution of ions around the RNA, they also both determine the nature of the counterion-induced compact states of RNA. Thus, the natural variable that controls RNA stability is the charge density  $\zeta = Ze/V$  where  $Ze$  is the charge and  $V$  is the volume of the cation.

In accord with the arguments given above, we previously reported that small metal ions stabilized near-native conformations of the *Tetrahymena* ribozyme more effectively than large cations of the same valence.<sup>16</sup> Similarly, we showed, using experiments and simulations, that when the ribozyme was refolded in polyamines, small multivalent polyamines stabilized the folded RNA more effectively than large diamines or ammonium ion.<sup>17</sup> Because the hydration chemistry of polyamines does not change significantly with their size, it is unlikely that such effects are due to bond energy or coordination geometry. Instead, we inferred that  $\zeta$  of the counterions is important for RNA folding, as has been suggested for DNA condensation.<sup>18–20</sup> Here, we reveal similar trends among divalent metal ions, under low salt conditions in which the association of counterions with the RNA is dominated by polyelectrolyte effect. We further establish that these effects require only nonspecific ion condensation using Brownian dynamics simulations of strongly charged polyelectrolytes that show that compaction and the energy of the collapsed state are determined by  $\zeta$ .

## Results

**Size of Metal Ions.** To determine the extent to which the size of hydrated cations changes the stability of RNA tertiary structure, the folding equilibrium of the *Tetrahymena* ribozyme was compared in  $\text{MgCl}_2$ ,  $\text{CaCl}_2$ ,  $\text{SrCl}_2$ , and  $\text{BaCl}_2$ . Among the group IIA ions, only  $\text{Mg}^{2+}$  supports the ribozyme's catalytic activity.<sup>21</sup> All these metal ions, however, stabilize native-like intermediates ( $I_N$ ) of the *Tetrahymena* ribozyme which readily convert to the native (N) RNA in the presence of  $\text{Mg}^{2+}$  (Figure 1).<sup>16,22</sup> To measure the extent of folding, ribozyme RNA was equilibrated in 50 mM Na–Hepes plus various divalent metal ions at 30 °C. Native-like conformers were then captured in nondenaturing polyacrylamide gels containing 3 mM  $\text{MgCl}_2$ <sup>23</sup> and separated from more slowly migrating unfolded or mis-

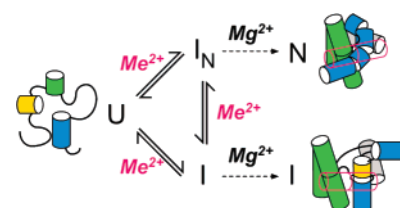


**Figure 1.** Folding mechanism of *Tetrahymena* ribozyme. U, unfolded RNA in low ionic strength; I, misfolded intermediates;  $I_N$ , native-like intermediates that can form in a counterion; N, native ribozyme that is formed in  $\text{Mg}^{2+}$ . Adapted from ref 16.

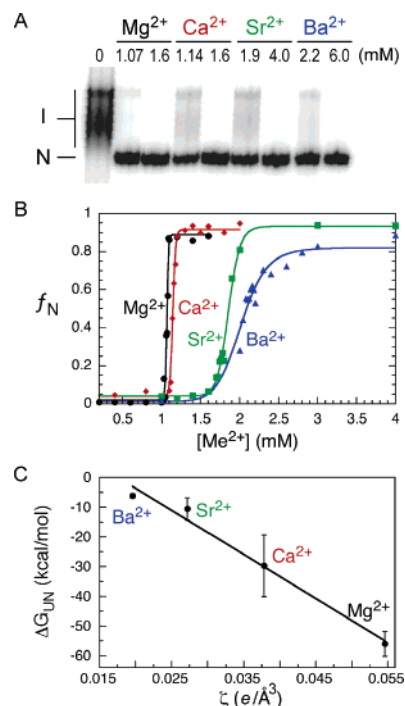


**Figure 2.** Folding of *Tetrahymena* ribozyme by group IIA metal ions. Folding reactions were in 50 mM Na–Hepes, pH 7.5, 1 mM EDTA (HE), 10% (v/v) glycerol, 0.01% xylene cyanol plus metal chloride at 30 °C. (a) Sample native 8% polyacrylamide gel. The ribozyme was folded in the concentrations of  $\text{MgCl}_2$ ,  $\text{CaCl}_2$ ,  $\text{SrCl}_2$ , or  $\text{BaCl}_2$  shown above each lane. I is the misfolded RNA, N is the native RNA. (b) Fraction of native RNA ( $f_N$ ) versus cation concentration. Curves represent the best fit to the Hill equation, with the parameters given in Table 1. (c) Folding free energy of the *Tetrahymena* L-21Sca ribozyme ( $\Delta G_{UN}(\text{Me})$ ) vs cation charge density ( $\zeta$ ).  $\Delta G_{UN}(\text{Me})$  was taken from the cooperativity of the transitions in (b).<sup>23</sup> Error bars are the variation in two independent trials. For each ion,  $\zeta$  was calculated from the volume of a sphere with radius equal to the length of the metal–oxygen bond.

folded conformers (I; Figure 2A). The gels were run at  $\leq 10$  °C to inhibit refolding of the RNA during electrophoresis.

When folding reactions in group IIA metal ions were compared, the midpoint of folding increased with the size of the cation, while the cooperativity of the transition decreased (Figure 2B and Table 1). The free energy difference between the unfolded and folded RNA ( $\Delta G_{UN}(\text{Me})$ ) in saturating metal ion (Me) was calculated from the cooperativity of the folding transition.<sup>23</sup> Remarkably,  $\Delta G_{UN}(\text{Me})$  decreased linearly with the charge density  $\zeta$  of the metal ion (Figure 2C). Hence, the ribozyme is more stable in smaller divalent metal ions such as  $\text{Mg}^{2+}$ , consistent with hydroxyl radical footprinting of the ribozyme tertiary interactions.<sup>24</sup>

- (13) Manning, G. S. *Q. Rev. Biophys.* **1978**, *11*, 179.  
 (14) Bloomfield, V. A. *Biopolymers* **1997**, *44*, 269.  
 (15) Grosberg, A. Y.; Nguyen, T. T.; Shklovskii, B. I. *Rev. Modern Phys.* **2002**, *74*, 329.  
 (16) Heilman-Miller, S. L.; Thirumalai, D.; Woodson, S. A. *J. Mol. Biol.* **2001**, *306*, 1157.  
 (17) Koculi, E.; Lee, N. K.; Thirumalai, D.; Woodson, S. A. *J. Mol. Biol.* **2004**, *341*, 27.  
 (18) Rouzina, I.; Bloomfield, V. A. *J. Phys. Chem.* **1996**, *100*, 4305.  
 (19) Stigter, D.; Dill, K. A. *Biophys. J.* **1996**, *71*, 2064.  
 (20) Tan, Z. J.; Chen, S. J. *Biophys. J.* **2006**, *90*, 1175; Tan, Z. J.; Chen, S. J. *Biophys. J.* **2006**, *91*, 518.  
 (21) McConnell, T. S.; Herschlag, D.; Cech, T. R. *Biochemistry* **1997**, *36*, 8293; Grosshans, C. A.; Cech, T. R. *Biochemistry* **1989**, *28*, 6888.  
 (22) Celander, D. W.; Cech, T. R. *Science* **1991**, *251*, 401.

- (23) Pan, J.; Thirumalai, D.; Woodson, S. A. *Proc. Natl. Acad. Sci. U.S.A.* **1999**, *96*, 6149.

**Table 1.** Group IIA Metal Ion Folding of the *Tetrahymena* Ribozyme

cation	M–O <sup>a</sup> (Å)	$n_{MO}^b$	$\xi^c$ (e/Å <sup>3</sup> )	$C_m^d$ (mM)	$n_H^e$	$\Delta G_{UN}(Me)^f$ (kcal/mol)
Mg <sup>2+</sup>	2.07	6	0.055	1.04 ± 0.04	98 ± 10	−56 ± 4
Ca <sup>2+</sup>	2.33	6	0.038	1.16 ± 0.02	66 ± 1	−30 ± 10
Sr <sup>2+</sup>	2.66	7.9	0.027	1.87 ± 0.01	19 ± 7	−10 ± 4
Ba <sup>2+</sup>	2.99	9.5	0.020	2.00 ± 0.03	11 ± 2	−6.2 ± 0.7

<sup>a</sup>Length of metal oxygen bond.<sup>51</sup> Fully hydrated ions are larger due to contributions from hydrogen atoms and additional water layers. <sup>b</sup>Number of water ligands.<sup>51</sup> <sup>c</sup>Charge density of metal cations were calculated by dividing the charge of the cation by its volume. The volume of hydrated cations was calculated as the volume of a sphere with a radius equal to the length of metal oxygen bond. <sup>d</sup>Midpoint of the folding transition from the fit of equilibrium data to the Hill equation (see Figure 2B). The error is the deviation for two independent data sets. <sup>e</sup>Hill coefficient; the error is the deviation for two independent data sets. <sup>f</sup>Maximum free energy gap between the unfolded and folded RNA,  $\Delta G_{UN}(Me)$  was calculated from the cooperativity of the folding transition at 30 °C,  $\Omega_C$ , as previously described.<sup>23</sup> The error is the deviation from the mean of two independent data sets.

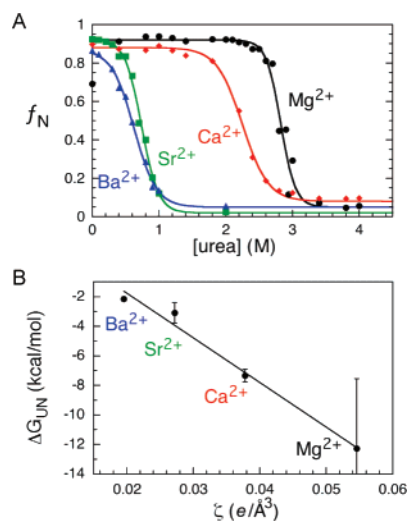
**Table 2.** Urea Denaturation of *Tetrahymena* Ribozyme

cation	$D_m^a$ (M)	$m^b$ (kcal mol <sup>−1</sup> M <sup>−1</sup> )	$\Delta G_{UN}(urea)^c$ (kcal/mol)
Mg <sup>2+</sup>	2.89 ± 0.09	4.3 ± 1.8	−12.3 ± 4.7
Ca <sup>2+</sup>	2.26 ± 0.01	3.3 ± 0.2	−7.3 ± 0.4
Sr <sup>2+</sup>	0.62 ± 0.17	5.0 ± 0.3	−3.1 ± 0.7
Ba <sup>2+</sup>	0.51 ± 0.16	4.4 ± 1.1	−2.2 ± 0.1

<sup>a</sup>Midpoint of urea unfolding transition from the native gel data (see Figure 3A). The RNA was folded at 30 °C in HE buffer and 3 mM MeCl<sub>2</sub>. <sup>b</sup>Constant that relates the free energy of unfolding to the concentration of urea. <sup>c</sup> $\Delta G_{UN}(urea)$  in 3 mM MeCl<sub>2</sub> was determined by urea denaturation and linear extrapolation to zero denaturant.

**Urea Denaturation.** To determine whether ion size changes the stability of the RNA tertiary interactions, we also measured the stability of RNA folded in 3 mM each cation by urea denaturation (Figure 3A).<sup>25,26</sup> We again observed a decrease in  $\Delta G_{UN}(urea)$  with increasing charge density  $\zeta$ , of the metal cation (Figure 3B). This is also reflected in a 4–5-fold drop in the midpoint of the urea denaturation curve in 3 mM Mg<sup>2+</sup> versus 3 mM Ba<sup>2+</sup> but little change in the slope or  $m$ -value (Figure 3A). If the  $m$ -value correlates with the surface area exposed upon unfolding,<sup>25</sup> these results suggest that the folded ribozyme is approximately as compact in any of these metal ions, in agreement with relatively small differences in the radius of gyration in Mg<sup>2+</sup> and Ca<sup>2+</sup> measured by small-angle X-ray scattering.<sup>27</sup> That the average conformation of the folded ensemble is roughly similar does not mean that the RNA has the same energetic stability—dynamic fluctuations, for example, may differ considerably in the various metal ions.

The magnitude of  $\Delta G_{UN}(urea)$  measured by urea denaturation was much smaller than the free energy gap estimated from the ion titration (−12 vs −55 kcal/mol in Mg<sup>2+</sup>). One explanation for this discrepancy is that RNA denatured in urea remains more structured and at a lower free energy than “unfolded” RNA in 50 mM Na–Hepes. This argument is supported by preliminary SAXS measurements showing that the related *Azoarcus* group I ribozyme is much less unfolded in 6 M urea plus 3 mM MgCl<sub>2</sub> than in buffer with no Mg<sup>2+</sup>,<sup>28</sup> consistent with a smaller free

(24) Celander, D. W.; Cech, T. R. *Science* **1991**, *251*, 401.(25) Shelton, V. M.; Sosnick, T. R.; Pan, T. *Biochemistry* **1999**, *38*, 16831.(26) Pace, C. N. The stability of globular proteins. In *CRC Critical Reviews in Biochemistry*, ed.; Chemical Rubber Company: Cleveland, OH, 1975; Vol. 3, p 1.(27) Russell, R.; Millett, I. S.; Doniach, S.; Herschlag, D. *Nat. Struct. Biol.* **2000**, *7*, 367.

**Figure 3.** Urea denaturation of the *Tetrahymena* ribozyme. (a) Ribozyme RNA folded in HE plus 3 mM MgCl<sub>2</sub>, CaCl<sub>2</sub>, SrCl<sub>2</sub>, or BaCl<sub>2</sub> at 30 °C was denatured with the addition of 0–5 M urea. The fraction of folded RNA,  $f_N$ , was measured by native PAGE and fit to the linear extrapolation model as described in Methods and Table 2. (b) Correlation of the folding free energy in water extrapolated from the urea denaturation curves ( $\Delta G_{UN}(urea)$ ) with  $\zeta$ .

energy difference between the native and urea denatured states. We have also observed a similar difference in the extent to which P5abc RNA is unfolded in urea plus Mg<sup>2+</sup> and in low salt buffer with no Mg<sup>2+</sup>.<sup>29</sup>

**Small Divalent Metals Induce More Compact RNA Structures.** Our previous work on the folding dynamics of the *Tetrahymena* ribozyme in various counterions suggested that ions with low charge density produce RNA conformational ensembles that are structurally broader and more dynamic than high charge density counterions.<sup>30,31</sup> To determine whether the size of divalent metal ions influences the average compactness of the ribozyme, we compared the electrophoretic mobility of the RNA in gels containing MgCl<sub>2</sub>, CaCl<sub>2</sub>, and SrCl<sub>2</sub>. The migration of nucleic acids in polyacrylamide gels is a complex function of mean end-to-end distance, chain conformation, and flexibility.<sup>32</sup> In general, folded RNAs with a smaller hydrodynamic radius migrate more rapidly through the gel than less tightly folded RNAs.<sup>33</sup> On the other hand, even small differences in flexibility can cause large changes in the electrophoretic mobility of DNA.<sup>34</sup>

The mobility of the unfolded and pre-folded ribozyme was measured relative to double-stranded  $\Phi$ X/Hae III DNA markers in non-denaturing 8% polyacrylamide gels containing either 3 mM MgCl<sub>2</sub>, CaCl<sub>2</sub> or SrCl<sub>2</sub> in the running buffer (Figure 4A). Under all conditions, the folded RNA migrated more rapidly than the unfolded RNA, as expected. Moreover, the folded RNA

(28) Chauhan, S.; Caliskan, G.; Briber, R. M.; Thirumalai, D.; Woodson, S. A.; Unpublished data.

(29) Koculi, E. Cation interactions in the RNA folding landscape. Ph.D. Thesis, Johns Hopkins, Baltimore, 2005.

(30) Heilman-Miller, S. L.; Pan, J.; Thirumalai, D.; Woodson, S. A. *J. Mol. Biol.* **2001**, *309*, 57.(31) Koculi, E.; Thirumalai, D.; Woodson, S. A. *J. Mol. Biol.* **2006**, *359*, 446.(32) Zimm, B. H.; Levene, S. D. *Q. Rev. Biophys.* **1992**, *25*, 171; Haran, T. E.; Cohen, I.; Spasic, A.; Yang, K.; Mohanty, U. *J. Am. Chem. Soc.* **2003**, *125*, 11160.(33) Buchmueller, K. L.; Webb, A. E.; Richardson, D. A.; Weeks, K. M. *Nat. Struct. Biol.* **2000**, *7*, 362; Schultes, E. A.; Spasic, A.; Mohanty, U.; Bartel, D. P. *Nat. Struct. Mol. Biol.* **2005**, *12*, 1130.(34) Olson, W. K.; Marky, N. L.; Jernigan, R. L.; Zhurkin, V. B. *J. Mol. Biol.* **1993**, *232*, 530.



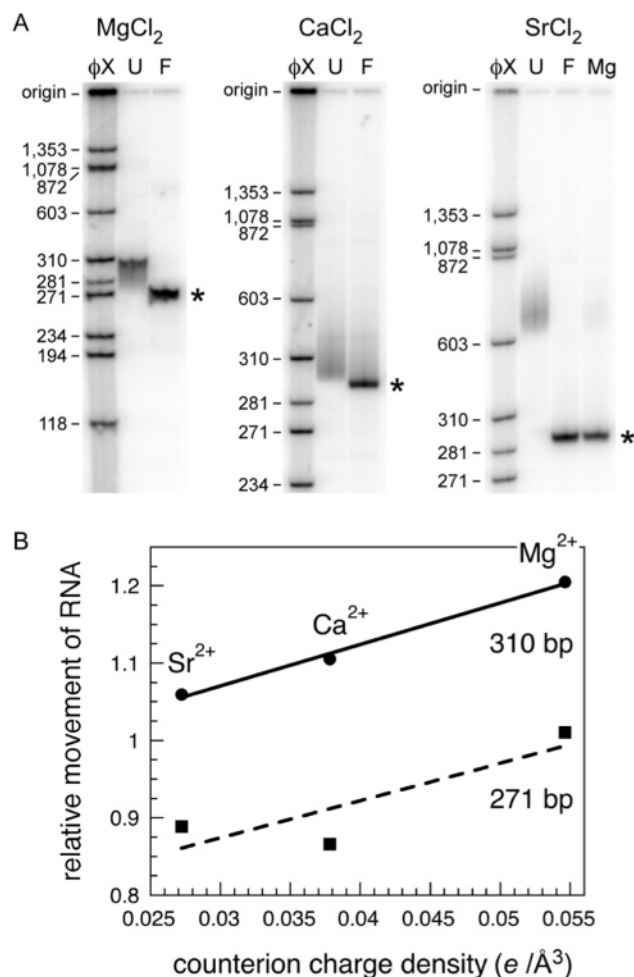


**Figure 4.** Relative gel mobility of ribozyme decreases with metal ion size. (a) Native 8% PAGE of the unfolded (U) or folded (F) *Tetrahymena* ribozyme, in running buffer containing 3 mM metal chloride (see Methods). The unfolded ribozyme samples were in HE buffer, the folded RNA was in HE plus 1.4 mM MgCl<sub>2</sub>, 1.4 mM CaCl<sub>2</sub>, or 6 mM SrCl<sub>2</sub>, respectively.  $\Phi X$ , 5'-<sup>32</sup>P-labeled  $\Phi X/Hae$  III DNA. (b) Relative mobility of the folded ribozyme compared to the 271 or 310 bp DNA, as a function of counterion charge density ( $\zeta$ ). Similar results were obtained in two trials.

traveled furthest relative to the 310 and 271 bp DNA fragments when the electrophoresis buffer contained 3 mM MgCl<sub>2</sub>. Overall, the relative mobility of the folded ribozyme decreased with the charge density of the metal ion, with Mg<sup>2+</sup> > Ca<sup>2+</sup> > Sr<sup>2+</sup> (Figure 4B). These results are consistent with either more compactly folded or less flexible structures in Mg<sup>2+</sup> compared with Ca<sup>2+</sup> or Sr<sup>2+</sup>.

To assess which of these two factors contributed most to the variation in gel mobility, we also measured the average Stokes radius of the *Tetrahymena* ribozyme by gel filtration chromatography, which yielded  $R_H \approx 43$  Å in 3 mM MgCl<sub>2</sub> (data not shown). Similar values ( $\pm 3\%$ ) were obtained for the ribozyme in 3 mM CaCl<sub>2</sub>, SrCl<sub>2</sub> and BaCl<sub>2</sub>, although the elution peak was broader in SrCl<sub>2</sub> and BaCl<sub>2</sub>. Together with the native gel mobility measurements, these data are consistent with a more dynamic ensemble of structures in the larger ions but a similar Stokes radius for the folded ribozyme.

**Temperature-Dependence of Folding.** Remarkably, the dependence of the folding free energy on ion size begins to disappear as the temperature of the ribozyme folding reaction approaches the  $T_m$  (65 °C in Mg<sup>2+</sup>;<sup>35</sup>) (Figure 5). Titrations with

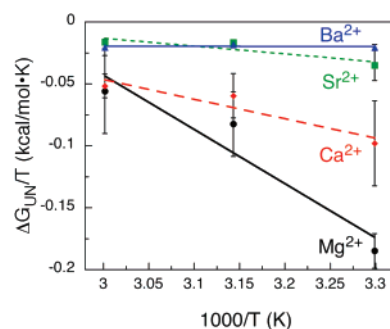


**Figure 5.** Temperature dependence of folding in group IIA metals.  $\Delta G_{UN}$  (Me) was measured by titration with MeCl<sub>2</sub> at 30, 45, and 60 °C as in Figure 2. Curves represent the best fit line. Error bars represent the variation in two or more trials.

the various metal ions were carried out as in Figure 2. In contrast with folding reactions in Mg<sup>2+</sup> and Ca<sup>2+</sup>, which depend steeply on temperature, the temperature dependence of the folding equilibrium in Sr<sup>2+</sup> and Ba<sup>2+</sup> was weak. Thus, at 60 °C, the folding free energy is only  $\sim 10$  kcal/mol lower in Mg<sup>2+</sup> and Ca<sup>2+</sup> compared with Sr<sup>2+</sup> and Ba<sup>2+</sup>. The curvature in the van't Hoff plot for Mg<sup>2+</sup> and Ca<sup>2+</sup> may be due to greater stability of folding intermediates (I) in these ions or a change in heat capacity. However, the latter would require values of  $\Delta C_p$  for RNA tertiary folding larger than those reported to date ( $+0.7$  to  $-3.4$  kcal/mol·K).<sup>36</sup>

**Simulation of Collapse Dynamics in Divalent Cations.** The dependence of  $\Delta G_{UN}$  on  $\zeta$  that we observe in Figures 2 and 3 can be explained either by (1) nonspecific interactions among cations and with the RNA or (2) specific coordination chemistry. The latter includes both hydration and direct coordination of the RNA by metal ions. Nonspecific effects include Coulomb interactions between cations and RNA, which are weaker for larger ions. Nonspecific effects also include the excluded volume of the cations, and ion–ion correlations. Because these interactions are generic for all RNAs, we refer to them collectively as the “polyelectrolyte effect”. We carried out coarse-grained simulations to evaluate the extent to which RNA collapse transitions depend on ion size, in the absence of hydration and specific coordination.

Using a simple bead-spring model for a polyelectrolyte (Materials and Methods), we generated eight trajectories for each divalent cation with the hydrodynamic radius of the cation varying from  $R_{ion} = 2.07, 2.33, 2.61, 2.99$  Å to simulate the collapse dynamics (Figure 6A). The counterion-mediated collapse of the polyelectrolyte chain was initiated at  $t \approx 0.1$   $\mu$ s by changing  $\epsilon$  from 0.5 to 2.0  $RT$ , which induces chain collapse by altering the solvent quality. The initial rise in the square of the radius of gyration ( $R_g^2(t) = 1/2N^2 \sum_{ij} r_{ij}^2$ ) when  $\epsilon = 0.5$   $RT$  is due to the electrostatic repulsion between the monomers. Upon increasing  $\epsilon$  to 2.0  $RT$ , counterion-mediated collapse of the polyelectrolyte leads to the rapid formation of pearl-necklace structures, which coalesce to form compact globules at long times (Figure 6A). The simulation results show that the smaller ions are more effective in driving the collapse of the polyelectrolyte. The total energy value of the final collapsed structure

(35) Banerjee, A. R.; Jaeger, J. A.; Turner, D. H. *Biochemistry* **1993**, *32*, 153.  
 (36) Fang, X. W.; Golden, B. L.; Littrell, K.; Shelton, V.; Thiyagarajan, P.; Pan, T.; Sosnick, T. R. *Proc. Natl. Acad. Sci. U.S.A.* **2001**, *98*, 4355; Mikulecky, P. J.; Feig, A. L. *Nucleic Acids Res.* **2004**, *32*, 3967; Hammann, C.; Cooper, A.; Lilley, D. M. *Biochemistry* **2001**, *40*, 1423; Klostermeier, D.; Millar, D. P. *Biochemistry* **2000**, *39*, 12970.

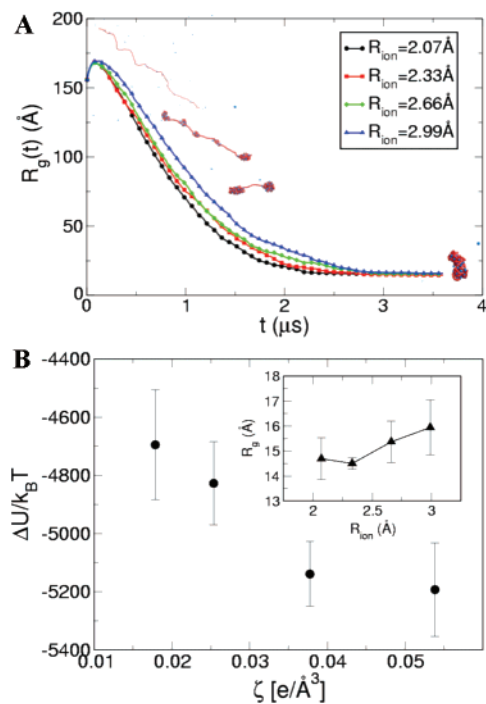


**Figure 6.** Simulation of polyelectrolyte collapse by small and large metal ions. (a) The collapse dynamics of a model polyelectrolyte ( $N = 120$ ) in divalent counterions of various sizes is shown as the change in the radius of gyration ( $R_g$ ) with time. Each time trace is averaged over eight individual trajectories to minimize the statistical errors. (b) Internal energy of the collapsed state of the polyelectrolyte, for four different counterions. (Inset)  $R_g$  of the collapsed polyelectrolyte as a function of the hydrodynamic radius of the counterion ( $R_{ion}$ ).

as a function of charge density ( $\zeta = 2e/(4\pi/3)R_{ion}^3$ ) shows similar trend as the  $\Delta G_{UF}$  vs  $\zeta$  plot obtained for RNA (Figure 6B), although the final compactness of the RNA increases only slightly from  $Mg^{2+}$  to  $Ba^{2+}$  (see inset). Furthermore, the simulations support our assertion that  $\zeta$ , rather than specific metal ion coordination, determines RNA stability. In other words, the observed linear relation between  $\Delta G$  and  $\zeta$  is due to the polyelectrolyte effect.

The variation in stability of the collapsed globule is not due to the extent to which backbone charges are neutralized. Upon condensation of the cations, the backbone charge is reduced by about 85%, independent of the size of the ions. The origins of the observed link between RNA stability and counterion charge density are most clearly reflected in the radial distribution function  $g(r)$  of the distances between the divalent ions and the charged monomers (Figure 7A) and the correlation  $g(r)$  between the condensed counterions (Figure 7B). The distance of closest approach of the ions to the polymer increases as their radii increase (Figure 7A). In addition, the smaller condensed ions are more highly correlated (see pronounced peaks at shorter distances in Figure 7B), due to a smaller excluded volume. Although these correlations do not significantly change the  $R_g$  of the collapsed state, they affect the stability of the folded RNA greatly, as observed in the experiments and simulations.

## Discussion

The distribution of counterions in the electrostatic field of the RNA has been successfully modeled by the mean field Poisson–Boltzmann theory<sup>4</sup> or the mechanism based on counterion condensation.<sup>13,14,37</sup> Because these models do not take

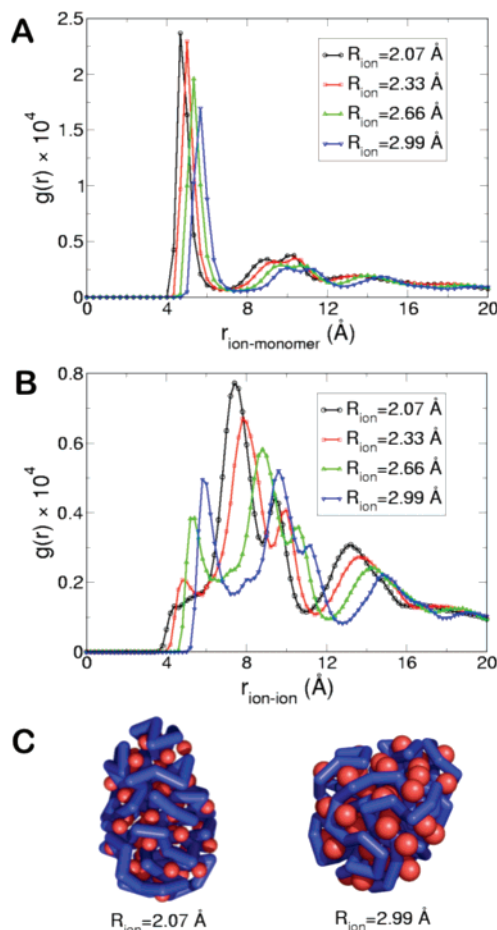


**Figure 7.** Ion-monomer distance distribution and correlations between condensed ions. (a) Radial distribution of the distances between the divalent ions and a model polyelectrolyte. (b) Pair correlation between ions that are condensed around the model polyelectrolyte. The correlation effects are reflected in the packing of the divalent around the compact state. (c) Compact globules in ions the size of  $Mg^{2+}$  ( $R_{ion} = 2.07 \text{ \AA}$ ) and  $Ba^{2+}$  ( $R_{ion} = 2.99 \text{ \AA}$ ). The volume of the globule in  $Ba^{2+}$  is nearly 30% larger than the one in  $Mg^{2+}$ .

into account the size or shape of the counterions, however, they cannot predict the differences in the stability of the RNA in divalent cations that we observe. Our observation that the stability of RNA tertiary structure depends on the counterion charge density demonstrates the need for models which capture correlations among ions associated with nucleic acids.<sup>20,38</sup>

Because the coordination chemistry of the group IIA metals varies strongly with ionic radius, the effects of these ions on RNA structure and function are most often attributed to site-specific interactions between the ions and the RNA, which are very sensitive to coordination geometry and the energetic cost of dehydrating the metal ion.<sup>12,39</sup> Specific metal ion–RNA interactions contribute to the stability (and conformational specificity) of the native ribozyme and likely account for some of the differences we observe.<sup>40</sup> On the other hand, relatively few metal ions are localized to specific sites within the

(37) Manning, G. S. *Biopolymers* **2003**, *69*, 137.

(38) Ha, B. Y.; Thirumalai, D. *Macromolecules* **2003**, *36*, 9658; Tan, Z. J.; Chen, S. J. *J. Chem. Phys.* **2005**, *122*, 44903.

(39) Serra, M. J.; Baird, J. D.; Dale, T.; Fey, B. L.; Retatagos, K.; Westhof, E. *RNA* **2002**, *8*, 307.

(40) Johnson, T. H.; Tijerina, P.; Chadee, A. B.; Herschlag, D.; Russell, R. *Proc. Natl. Acad. Sci. U.S.A.* **2005**, *102*, 10176; Stahley, M. R.; Strobel, S. A. *Science* **2005**, *309*, 1587.

*Tetrahymena* ribozyme,<sup>8,41</sup> compared with the ~200 divalent ions needed to neutralize its negative charge. Moreover, the energetic cost of removing water from site-bound metal ions offsets much of their favorable Coulomb energy.<sup>42</sup> Thus, nonspecific “polyelectrolyte” effects are expected to stabilize the global fold of the RNA more than site-specific metal ion interactions.<sup>42</sup>

Our simulations, which completely ignore chemical details, show that the greater stability of the RNA in small metal ions can be explained in terms of polyelectrolyte effects, without invoking direct or indirect coordination of metals. Small ions are also more effective than large ions in DNA condensation, and this difference has also been attributed to polyelectrolyte effects.<sup>18,43</sup> Small, high charge density cations interact more favorably with the folded RNA, because they approach the RNA more closely (stronger attractive Coulomb interactions), and because the excluded volume of each ion is smaller.<sup>18,19</sup> The latter lowers the entropic penalty for confining the ions to a small volume around the RNA. In addition, high charge density cations are predicted to increase the attraction between charged helices, which may further stabilize the folded RNA.<sup>20,44</sup> The different hydration energies of the group IIA metals may affect their interactions with specific sites in the RNA, but our simulations show that such interactions are not needed to explain the increase in RNA stability with the decrease in metal ion radius.

## Conclusion

The collapse of the highly charged RNA molecule is determined by the extent to which the charges on the phosphate groups can be neutralized.<sup>16</sup> Charge neutralization in turn depends not only on the ion-RNA interaction but also on how close the nonspecific condensed counterions can approach each other.<sup>14,20,45</sup> The simplest variable that accounts for both electrostatic interactions and the excluded volume effects between cations is the charge density,  $\zeta$ . The simulations show that the remarkable linear correlation between stability of RNA and  $\zeta$  is largely due to the polyelectrolyte effect, not specific coordination of ions by RNA. The present work and our previous results on ribozyme folding in polyamines<sup>17,31</sup> show that the shape and size of the cations, that determine the packing of condensed ions, must be taken into account to describe the stability of RNA tertiary structures.

## Experimental Methods

**Ion-Dependence of Folding.** Folding of the L-21Sca ribozyme was measured by native PAGE as previously described.<sup>23</sup> Reactions were in 50 mM Na-Hepes, pH 7.5, 1 mM EDTA (HE), 10% (v/v) glycerol, 0.01% xylene cyanol plus various concentrations of metal chloride salts at 30 °C (2–4 h). The fraction of folded RNA was determined from the counts in the native RNA band (N) divided by the total counts in each lane. The fraction of native RNA,  $f_N$ , versus cation concentra-

tion,  $C$ , was fit to  $f_N = f_{N,\max} \cdot C^{n_H}/(C^{n_H} + C_m^{n_H})$ , where  $f_{N,\max}$  is the maximum amount of folded RNA at saturation,  $C_m$  is the midpoint of the transition, and  $n_H$  is the Hill constant.

**Urea Denaturation.** Ribozyme RNA was pre-folded in HE plus 3 mM metal chloride as above, then incubated with 0–6 M urea at 30 °C before native PAGE. The fraction of native RNA ( $f_N$ ) was fit to

$$f_N = \frac{f_{N,\max} + f_{N,\min} \exp[-m(D_m - D)/RT]}{1 + \exp[-m(D_m - D)/RT]} \quad (1)$$

where  $D$  is the concentration of urea,  $D_m$  is the midpoint of the unfolding transition, and  $m$  is a constant.<sup>46</sup> Folding free energies were obtained by linear extrapolation,  $-\Delta G_{UN} = \Delta G_{NU} = \Delta G_{H_2O} - m[D]$ .

**Determination of Relative Gel Mobility.** To measure the relative gel mobility in various metal ions, <sup>32</sup>P-labeled RNA was incubated in HE with or without MgCl<sub>2</sub>, CaCl<sub>2</sub> or SrCl<sub>2</sub> at 30 °C as above, and loaded on the gel immediately.  $\Phi$ X/Hae III DNA markers (New England Biolabs) were labeled with  $\gamma$ -[<sup>32</sup>P]-ATP and T4 polynucleotide kinase. Native 8% (29:1) polyacrylamide gels were prepared in 66 mM Hepes, 34 mM Tris, 0.1 mM EDTA, and 3 mM MgCl<sub>2</sub>, CaCl<sub>2</sub>, or SrCl<sub>2</sub> and run for 3–4 h at 700 V, with the gel and running buffer chilled to 4–10 °C. BaCl<sub>2</sub> was not stable to electrophoresis under these conditions. Migration distances were measured from the origin of the gel.

**Gel Filtration Chromatography.** Ribozyme RNA 0.5 mL of 0.16  $\mu$ M RNA solution was applied to a gel filtration column (Hi Prep 16/60 Sephacryl S300 HR; Pharmacia) in HE plus 3 mM MgCl<sub>2</sub>, CaCl<sub>2</sub>, SrCl<sub>2</sub>, or BaCl<sub>2</sub> at room temperature at 0.5 mL/min. The void volume of the column was determined by the elution of blue dextran. The Stokes radius of the RNA was determined by comparison with the elution volume of protein standards (cytochrome C,  $R_H = 17.4$  Å; bovine serum albumin, 35 Å; and bovine carbonic anhydrase, 24.5 Å).<sup>47</sup>

**Brownian Dynamics Simulations.** Brownian dynamics simulations of 2:1 polyelectrolyte system were performed, using counterions with hydrodynamic radii that correspond to Group II divalent metal cations. The polyelectrolyte chains were represented as linear Gaussian chains consisting of  $N = 120$  monomers. Two consecutive monomers, that are at an equilibrium distance  $a$  (6 Å), are connected by a harmonic potential with a spring constant  $k = 80RT/a^2$  where  $RT = 0.6$  kcal/mol. Each monomer with van der Waals radius of  $a/2$  carries a charge of  $-1e$ .  $N/2$  ( $= 60$ ) divalent (+2e) counterions, which neutralize the entire system, were randomly distributed within a 600 Å cube (0.5 mM) to generate the initial configurations.

The interactions between monomers are given by the 12-6 Lennard Jones potential. A Coulomb potential, with the Bjerrum length  $l_B = 35$  Å, represents the interaction between the charges. The larger than the typical value of  $l_B = 7$  Å in water emphasizes the strength of the electrostatic interactions relative to thermal fluctuations. Because  $l_B$  merely sets the energy scale,<sup>48</sup> the precise value does not alter the relationship between the energy of the collapsed structure of the polyelectrolyte and the ion size. The energy function for the system is given as

$$H_{\text{sys}}(\{\vec{r}_i\}) = \sum_{i=1}^{N-1} \frac{k}{2} (r_{i,i+1} - a)^2 + \sum_{i < j} \left( \epsilon \left[ \left( \frac{\sigma_{ij}}{r_{ij}} \right)^{12} - 2 \left( \frac{\sigma_{ij}}{r_{ij}} \right)^6 \right] + RT l_B \frac{z_i z_j}{r_{ij}} \right) \quad (2)$$

The van der Waals radii ( $\sigma_{ij} = \sigma_i + \sigma_j$ ) and valences ( $z_i, z_j$ ) depend on the type of interaction. For example, for monomer-ion interactions we used the parameters  $\sigma_i = a/2$ ,  $\sigma_j = R_{\text{ion}}$ ,  $z_i = -1$ , and  $z_j = +2$ . We computed the electrostatics of the system using Ewald summation procedure of Adams and Dubey.<sup>49</sup> The equations of motion were

(41) Christian, E. L.; Yarus, M. *Biochemistry* **1993**, *32*, 4475; Juneau, K.; Podell, E.; Harrington, D. J.; Cech, T. R. *Structure* **2001**, *9*, 221.

(42) Misra, V. K.; Shiman, R.; Draper, D. E. *Biopolymers* **2003**, *69*, 118.

(43) Trend, B. L.; Knoll, D. A.; Ueno, M.; Evans, D. F.; Bloomfield, V. A. *Biophys. J.* **1990**, *57*, 829; Plum, G. E.; Arscott, P. G.; Bloomfield, V. A. *Biopolymers* **1990**, *30*, 631.

(44) Gronbech-Jensen, N.; Mashl, R. J.; Bruinsma, R. F.; Gelbart, W. M. *Phys. Rev. Lett.* **1997**, *78*, 2477.

(45) Rouzina, I.; Bloomfield, V. A. *J. Phys. Chem.* **1996**, *100*, 4292.

(46) Santoro, M. M.; Bolen, D. W. *Biochemistry* **1988**, *27*, 8063.

(47) Siegel, L. M.; Monty, K. J. *Biochim. Biophys. Acta.* **1966**, *112*, 346.

(48) Lee, N.; Thirumalai, D. *Macromolecules* **2001**, *34*, 3446.

(49) Adams, D. J.; Dubey, G. S. *J. Comput. Phys.* **1987**, *72*, 156.

integrated using

$$\vec{r}_i(t + \Delta t) = \vec{r}_i(t) - \frac{D_i \Delta t}{k_B T} \frac{\partial H_{\text{sys}}}{\partial \vec{r}_i} + \sqrt{6D_i \Delta t} \vec{\xi}_i(t) \quad (3)$$

where  $\xi_i(t)$  is the Gaussian random noise satisfying  $\langle \vec{\xi}_i(t) \cdot \vec{\xi}_i(t') \rangle = \delta_{ij} \delta(t - t')$ .<sup>50</sup> Diffusion coefficients,  $D_m = 1.0 \times 10^{-7}$  cm<sup>2</sup>/s and

(50) Ermak, D. L.; McCammon, J. A. *J. Chem. Phys.* **1978**, *69*, 1352.

(51) Ohtaki, H.; Radnai, T. *Chem. Rev.* **1993**, *93*, 1157.

$D = (a/2R_{\text{ion}}) \times D_m$  are assigned for the monomers and the counterions, respectively, based on the Stokes–Einstein relation. The integration time step is  $\Delta t \approx 0.36$  ps.

**Acknowledgment.** S.W. thanks B. Garcia-Moreno and D. Draper for helpful discussion. This work was supported by grants from the NIH (GM46686 to S.W.) and the NSF (CHE 05-14056 to D.T).

JA068027R